The cubic-to-rhombohedral phase transition of $Pb(Zn_{1/3}Nb_{2/3})O_3$: a high-resolution x-ray diffraction study on single crystals

2002 J. Phys.: Condens. Matter 14 7035

(http://iopscience.iop.org/0953-8984/14/29/305)

INSTITUTE OF PHYSICS PUBLISHING JOURNAL OF PHYSICS: CONDENSED MATTER

J. Phys.: Condens. Matter **14** (2002) 7035–7043 PII: S0953-8984(02)33496-9

The cubic-to-rhombohedral phase transition of $Pb(Zn_{1/3}Nb_{2/3})O_3$: a high-resolution x-ray diffraction study on single crystals

A Lebon[1], **H Dammak, G Calvarin and I Ould Ahmedou**

Structures, Propriétés et Modélisation des Solides, UMR 8580, CNRS—Ecole Centrale Paris, Grande Voie des Vignes, 92295 Châtenay-Malabry Cedex, France

E-mail: a.lebon@fkf.mpg.de

Received 6 February 2002, in final form 23 May 2002
Published 11 July 2002
Online at stacks.iop.org/JPhysCM/14/7035

Abstract

The cubic-to-rhombohedral (C–R) phase transition of the ferroelectric relaxor $Pb(Zn_{1/3}Nb_{2/3}O_3)$ is investigated by means of a high-resolution x-ray diffraction study on single crystals. The phase transition is diffuse and spreads over the temperature range $T_{CR} = 385 \pm 5$ K to $T_R = 325 \pm 5$ K. Below T_{CR}, the cubic phase transforms progressively into rhombohedral domains whose average size, about 60–70 nm in the [111] direction, remains unchanged as temperature is lowered, so no growth of the R-domains is observed. At T_R, the nanometric R-domains fully pave the crystal but structural mismatches between adjacent domains generate stresses, which increase as temperature is lowered. The anomalous broadening of diffraction peaks of the R-phase, which originates from size and strain effects, can be suppressed by applying a dc electric field, along the [111] direction, which transforms the polydomain state into a rhombohedral quasi-monodomain state.

1. Introduction

Relaxor ferroelectrics were first synthesized in the late 1950s and since that time they have attracted lots of attention because of the unusual behaviour of their dielectric permittivity [1]. In fact, they display a significant dielectric anomaly characterized by strong frequency dispersion. Many of these materials are lead-based perovskites with general formula $PbBB'O_3$ ($B = Mg^{2+}, Zn^{2+}, Ni^{2+}, Sc^{3+}, \ldots$; $B' = Nb^{5+}, Ta^{5+}, W^{6+}, \ldots$). The most well documented relaxor $Pb(Mg_{1/3}Nb_{2/3})O_3$ (PMN) retains a cubic structure on average down to 5 K and displays no macroscopic spontaneous polarization [2]. $Pb(Zn_{1/3}Nb_{2/3})O_3$ (PZN), which is isomorphous to PMN, exhibits also the dielectric behaviour of a relaxor ferroelectric, but it is characterized by

[1] Address for correspondence: Festkörperforshung, Max Planck Institut, 1, Heisenbergstrasse, 70569 Stuttgart, Germany.

a symmetry lowering towards a rhombohedral ferroelectric phase as shown in the early study of Yokomizo *et al* [3]. The cubic-to-rhombohedral (C–R) phase transition which occurs around $T = 390$ K does not coincide with the maximum of the dielectric permittivity ($T_{max} = 405$ K, $f = 1$ kHz) [4]. From optical observations carried out on single crystals, Mulvihill *et al* [5] showed that the ferroelectric phase of PZN appears in a so-called microdomain state (<100 nm), which transforms into a macrodomain state under a dc electric field parallel to [111]. Moreover, from structural refinements of powder neutron diffraction patterns, Iwase *et al* [6] showed that the best results were obtained by assuming the coexistence of both cubic and rhombohedral phases below 550 K. The rhombohedral phase ratio reaches 40% at room temperature. On the other hand, Raman scattering experiments carried out on PZN single crystal by Lebon *et al* [7] did not give evidence of phase coexistence above 390 K; however, below this temperature a drastic increase of the intensity ratio $I_\perp / I_\parallel$ of the Raman bands was observed and associated with the onset of a rhombohedral microdomain state.

In order to achieve a better characterization of the C–R phase transition of PZN, an x-ray diffraction study was carried out on single crystals by means of a high-resolution diffractometer.

2. Experimental conditions

PZN single crystals were grown using a flux method with excess lead oxide. They were extracted from the flux with the aid of a warm 25% vol nitric acid solution [4, 8]. Three yellow transparent crystals were oriented and cut according to the crystallographic planes (100), (110) and (111) using the Laue technique. The crystals, accordingly $3 \times 2 \times 0.5$ mm^3 platelets, were polished on both surfaces, then annealed at 450 °C in order to remove residual stresses.

The x-ray diffraction diagrams were recorded with a high-accuracy two-axis diffractometer in Bragg–Brentano geometry built up in the laboratory [9]. Diffraction angles were measured with a relative precision better than 0.002° (2Θ) by means of a photoelectric encoder connected to the rotation axis of the diffractometer. A graphite monochromator selected the Cu Kβ wavelength ($\lambda = 0.139\,223$ nm) issued from an 18 kW rotating anode (Rigaku). Single crystals were fixed on a copper sample holder within a N_2 flow cryostat (230–470 K) mounted upon a HUBER goniometric head.

3. Results

Special care was taken to select Bragg reflections with high diffraction angles since they are more sensitive to any weak structural distortion. The (333), (330) and (005) reflections were selected and recorded from the three crystals respectively in the temperature range 450–241 K. Figure 1 shows plots at $T = 400$ and 300 K (RT). At RT, the peaks (333) and (330) are split while the peak (005) remains unique, which is consistent with a rhombohedral symmetry as already reported in the literature [3]. The anomalous broadening of peaks at RT, with respect to high temperature, will be discussed below. Figure 2 shows recordings of the (333) peak at six selected temperatures. Down to 400 K, the single peak (figure 2(a)) corresponds to the cubic phase. At $T = 370$ K, an asymmetry is observed on the left side of the peak (figure 2(a)), asymmetry which turns into a shoulder at $T = 351$ K (figure 2(b)). At lower temperatures, two very distinct peaks, corresponding to the rhombohedral doublet $(333)_R$ and $(-333)_R$, are clearly evidenced. The progressive splitting of (333) indicates that the spontaneous C–R phase transition of PZN is diffuse in temperature. The temperature dependence of the full width at quarter-maximum (FWQM) of (333) is shown in figure 3. This width was chosen instead of the FWHM since the $(333)_R$ component appears as a weak feature on the left side of the cubic

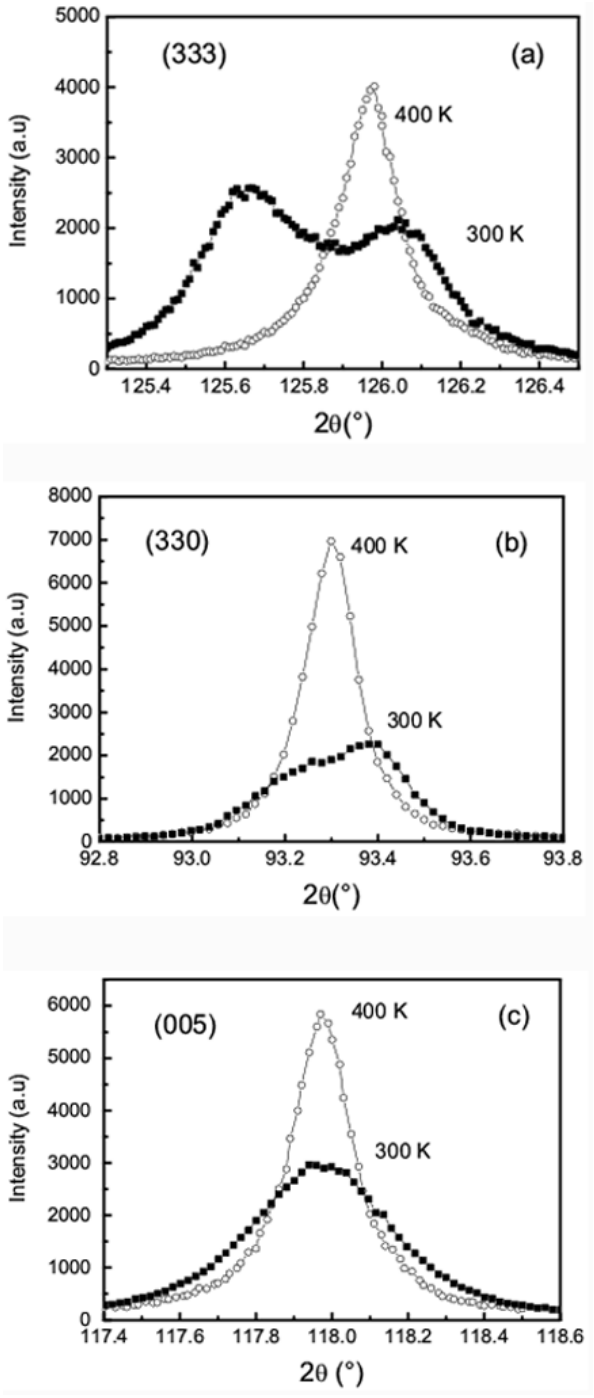

Figure 1. Diffraction patterns at temperatures of $T = 400$ and 300 K for three Bragg reflections: (a) (333), (b) (330) and (c) (005).

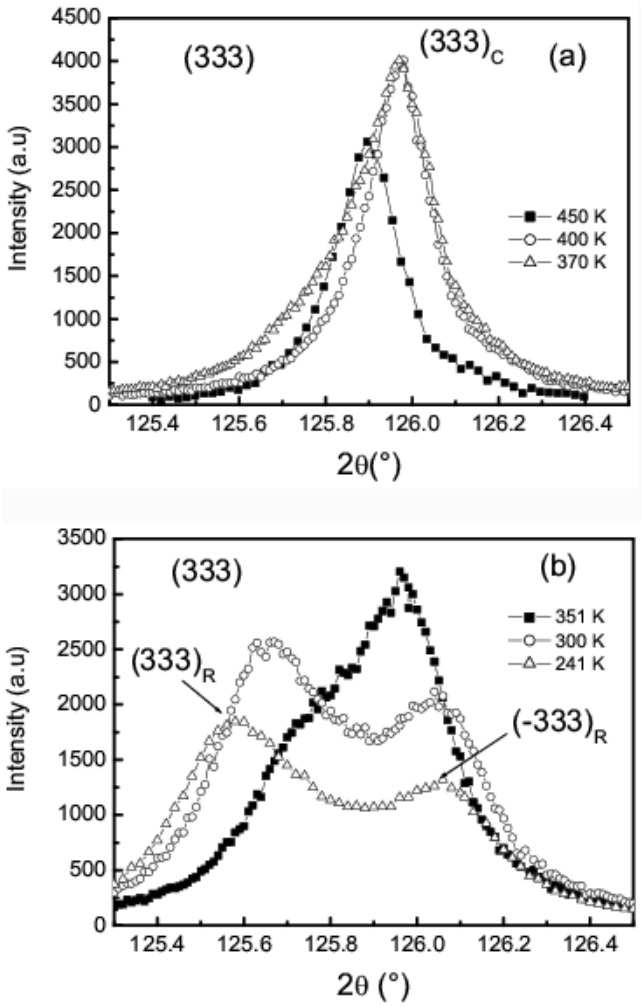

Figure 2. The temperature dependence of the diffraction peak (333) in the ranges (a) 450–370 K, (b) 351–241 K.

reflection. It is thus easier to determine the true transition temperature with a width that is more sensitive to the occurrence of the domain state. The FWQM slightly increases in the cubic phase, then it abruptly jumps. The slope change takes place at 385 ± 5 K. A similar behaviour is also observed for the temperature dependence of the full width at half-maximum (FWHM) of (005), (figure 3). So, $T_{CR} = 385 \pm 5$ K can be taken as the onset temperature of the C–R phase transition. In addition, a second slope change takes place at 325 ± 5 K, the significance of which will be discussed below.

In order to get further quantitative information about the structural features of the C–R phase transition, the (333) peak was fitted using pseudo-Voigt profile functions. Below T_{CR}, two components are fitted and the low-angle component is assigned to the R-peak $(333)_R$. The temperature dependences of intensities and FWHM are shown in figures 4(a) and (b) respectively. The intensity of the R-component $(333)_R$ increases throughout the whole temperature range below T_{CR}, as the intensity of $(333)_C$ does in the C-phase (figure 4(a)). On

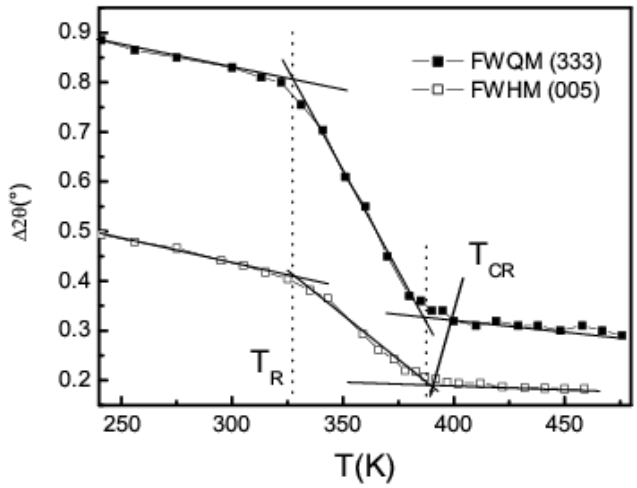

Figure 3. Temperature dependences of (333) (FWQM) and (005) (FWHM). Two slope changes are observed, at $T_{CR} = 385 \pm 5$ K and $T_R = 325 \pm 5$ K.

the other hand, the intensity of the high-angle component decreases from T_{CR} down to around 325 K and subsequently remains quasi-constant. The FWHM of the R-component $(333)_R$ is quasi-constant between T_{CR} and 325 K but is much higher than the $(333)_C$ one, 0.30° against 0.17°(2Θ) (figure 4(b)). However, in the temperature range T_{CR}–325 K, the FWHM of the high-angle component increases from 0.17° to 0.30°(2Θ). Below 325 K, the FWHM of the two components are equal and increase in a similar way (figure 4(b)). These temperature dependences reveal a behaviour change, at $T_R = 325 \pm 5$ K, which can be related to the end of the C–R phase transition. Thus, in the temperature range T_{CR}–T_R, the high-angle component is the resultant of a summation of the C-peak $(333)_C$ and the R-peak $(-333)_R$ which are closely superimposed. Just below T_{CR}, the contribution of the C-peak is predominant and the observed increase of the FWHM between T_{CR} and T_R can be assigned to the increase of the volume ratio of the rhombohedral with respect to the cubic phase. At T_{CR}, the $(-333)_R$ component is expected to have the same FWHM as the $(333)_R$ one, but these two widths are actually observed at T_R and below this temperature when the R-phase prevails.

The temperature dependence of the cell volume of PZN, derived from fits, is shown in figure 5. Again, a change of behaviour is observed in the temperature range T_{CR}–T_R. The volume of both the C-phase (above T_{CR}) and the R-phase (below T_R) decreases as temperature is lowered; however, the R-volume is higher, at T_{CR}, $\Delta V/V = 0.06\%$ (figure 5). Thus, the C–R phase transition of PZN is weakly first order, which is consistent with the observed phase coexistence in the temperature range T_{CR}–T_R; in this range the cell volume dependence is meaningless (figure 5).

4. Discussion

The temperature dependences of the intensity (figure 4(a)) and FWHM (figure 4(b)) of the R-peak $(333)_R$, between T_{CR} and T_R, suggest that the C-phase transforms progressively into nanometric R-domains quasi-constant in size. The average size along the [111] direction could be calculated by means of the Scherrer formula [10], assuming that the instrumental width is equal to the $(333)_C$ FWHM in the C-phase. The estimated size of 60–70 nm for the R-domains

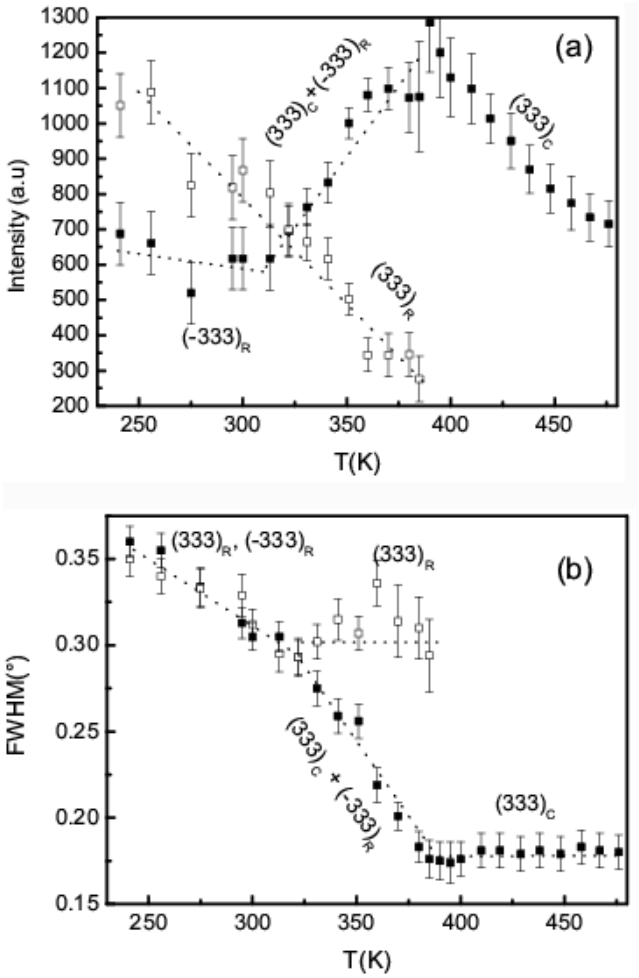

Figure 4. Temperature dependences of the intensities (a) and FWHM (b) of the $(333)_C$, $(333)_R$ and $(-333)_R$ peaks. The indices C and R stand for the cubic and the rhombohedral phases.

is in qualitative agreement with the optical observations of Mulvihill *et al* [5] who evidenced ferroelectric domains of <100 nm in size. The onset of nanometric R-domains within the C-matrix has also been observed in PMN. However, for this latter, the transformation is not spontaneous, but time dependent when a dc electric field is applied along a [111] direction below a temperature $T_g = 230$ K: i.e. in the so-called glassy phase of PMN [11]. Moreover, as for PZN, nanometric R-domains nucleate within the C-phase with a constant average size of 70 nm in the [111] direction [12][2].

At T_R the crystal is fully paved by nanometric R-domains, but stresses are generated inside the crystal because of structural mismatches between adjacent domains. Below T_R, structural mismatches increase correlatively to the rhombohedral distortion, as illustrated in figure 6 with the temperature dependence of rhombohedral angle α. Thus, below T_R a strain effect is superimposed on the size one which explains the increase in FWHM of both R-peaks $(333)_R$ and $(-333)_R$. The temperature dependence of the (005) FWHM (figure 3) can also be explained

[2] The wrong value of R-domain size reported in [11] arises from a mistake in the calculation [12].

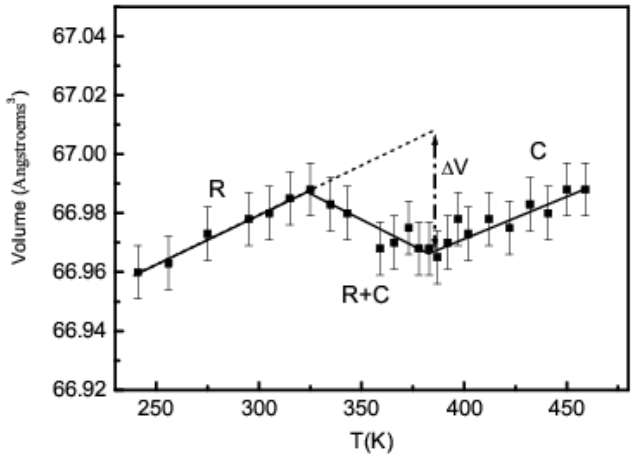

Figure 5. The temperature dependence of the cell volume of PZN.

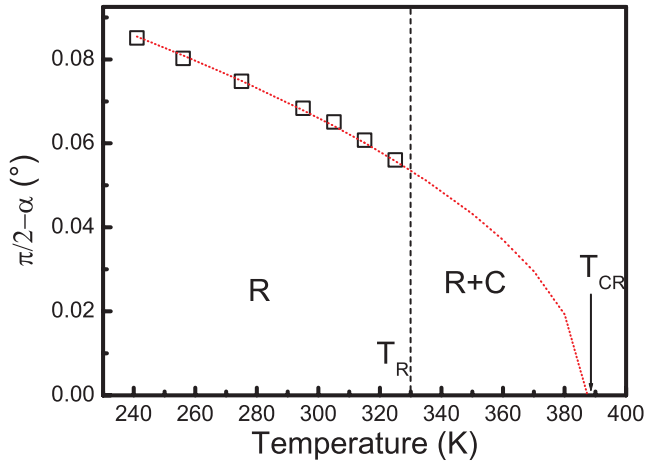

Figure 6. Rhombohedral distortion as a function of temperature below T_R.
(This figure is in colour only in the electronic version)

by the contribution of the two broadening effects. The broadening of R-phase peaks, generated by size and strain effects, can be suppressed by poling the crystal, under the condition that a sufficient electric field is applied along the direction of polarization [111] [13]. This process transforms the nanometric polydomain state into a macroscopic quasi-monodomain state as illustrated in figure 7 by the behaviour of the (333) Bragg reflection, where the R-peak $(333)_R$ is favoured by the dc electric field. This transformation of the domain state is accompanied by a decrease of both the $(333)_R$ and (005) FWHM that recover their value for the C-phase (figure 1). These results confirm that the anomalous broadenings associated with the spontaneous C–R phase transition arise from the existence of a nanometric polydomain state.

The temperature dependence of the depolarization ratio $I_\perp/I_\parallel$ of the Raman spectra of PZN was measured with the same single crystal as was used for the x-ray experiments [7]. This ratio was found to increase rapidly from T_{CR} to T_R, a temperature where it approaches unity. This behaviour was assigned as a signature of the onset of ferroelectric microdomains.

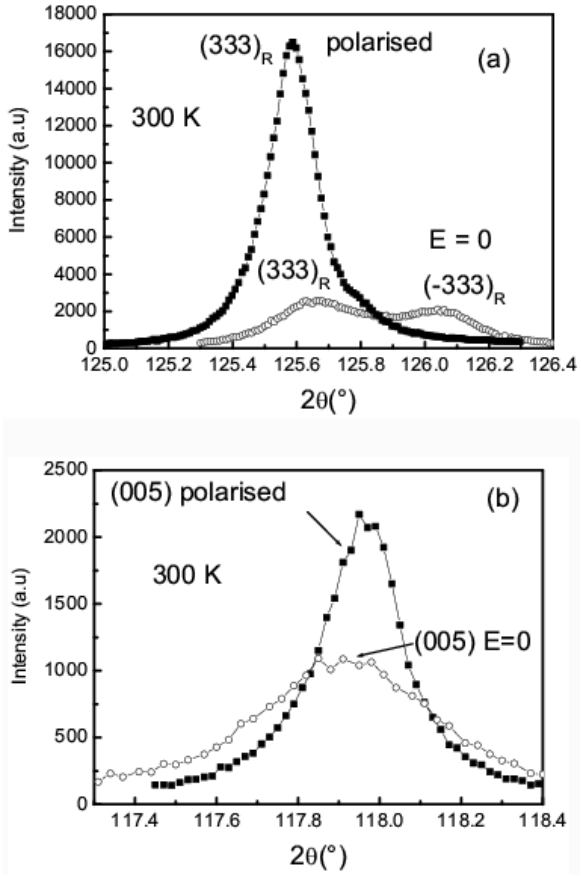

Figure 7. Recordings from the same crystal of (333) and (005) diffraction peaks before ($E = 0$) and after poling ($E = 3$ kV cm^{-1} at room temperature), with an applied electric field along [111].

5. Conclusions

In conclusion, our diffraction results reveal that the spontaneous C–R phase transition of PZN is first order and diffuse in temperature. The structural transformation takes place by a progressive nucleation of nanometric R-domains within the C-matrix, in the temperature range T_{CR}–T_R. The average size of R-domains remains unchanged over the whole temperature range investigated, so no growth of the R-phase is observed. The similar size lock-in observed in the first stage of the electric field-induced C–R phase transition of PMN has very probably a common origin. In fact, a recent x-ray investigation of PMN and PZN using a synchrotron source showed that chemically ordered regions exist in both compounds [14]. These ordered regions are the sources of quenched random fields, which might explain why the R-domains cannot grow over a few tens of nanometres.

References

[1] Smolensky G A *et al* 1961 *Sov. Phys.–Solid State* **2** 2584
[2] Bonneau P, Garnier P, Calvarin G, Husson E, Gavarri G R, Hewatt A W and Morell A 1991 *J. Solid State Chem.* **91** 350

[3] Yokomizo Y, Takahashi T and Nomura S 1970 *J. Phys. Soc. Japan* **28** 1278
[4] Ould Ahmedou I 1997 *PhD Thesis* Ecole Centrale de Paris
[5] Mulvihill M L, Cross L E, Cao W and Uchino K 1997 *J. Am. Ceram. Soc.* **80** 1462
[6] Iwase T, Tazawa H, Fujishiro K, Uesu Y and Yamada Y 1999 *J. Phys. Chem. Solids* **60** 1419
[7] Lebon A, El Marssi M, Farhi R, Dammak H and Calvarin G 2001 *J. Appl. Phys.* **89** 3947
[8] Mulvihill M L, Park S E, Risch G, Li Z and Uchino K 1996 *Japan. J. Appl. Phys.* **35** 3984
[9] Bérar J F, Calvarin G and Weigel D 1980 *J. Appl. Crystallogr.* **13** 201
[10] Guinier A 1964 *Théorie et Technique de la Radiocristallographie* (Paris: Dunod) p 462
[11] Vakhrushev S B, Kiat J-M and Dkhil B 1997 *Solid State Commun.* **103** 477
[12] Dkhil B 1999 *PhD Thesis* Université Paris XI
[13] Dammak H, Lebon A and Calvarin G 1999 *Ferroelectrics* **235** 151
[14] Fanning D M, Robinson I K, Lu X and Payne D A 2000 *J. Phys. Chem. Solids* **61** 209